SPE 114954

Simplifying Gas Production Modeling

Colin L. Jordan, SPE, and Robert Jackson, SPE, Boe Solutions Inc., and Cooper Smith, SemCAMS ULC

This paper was prepared for presentation at the CIPC/SPE Gas Technology Symposium 2008 Joint Conference held in Calgary, Alberta, Canada, 16–19 June 2008.

Abstract

This paper presents a simple, but reliable, method for predicting the performance of multiple gas wells in complex reservoir shapes. Using an approximation of the traditional "image well" method, pressure and production profiles can be generated for arbitrary shaped reservoirs, with internal boundaries and similar heterogeneity, as well as multiple well completions. The procedure will allow for modeling and analysis, as well as forecasting of complex operating conditions including varying rate and flowing pressure schedules (including shut-in) for conventional and unconventional gas systems without the need of advanced engineering mathematics or computational libraries.

The approach overcomes many limitations of conventional analytical methods (i.e. single well solutions or limited reservoir shapes) which are generally unsuitable for multi-well planning, in-fill drilling, or full field development. But, it also allows for petroleum engineers, without numerical simulation resources or skills, to perform field wide evaluations on reservoirs and wells with a variety of operating conditions. A number of computational and quality issues are addressed including Laplace space inversion methods; addition of wellbore storage and skin (at wellbore and observation points); incorporation of absorbed gas for unconventional gas systems; pressure dependant fluid properties; reservoir heterogeneity; and rate forecasting. The methodology is validated by comparison to both analytical solutions and commercial numerical tools.

In short, a new mathematical approach for production modeling and forecasting has been introduced. Mathematical adaptations for reservoir heterogeneity, complex reservoir shapes, multiple completions and rate forecasting are discussed. Adaptations and applications for both conventional and unconventional gas (including coal and shale gas) are demonstrated. Finally, a simple solution process is presented for quick and easy implementation in MS Excel or other common tools.

Introduction: General History & Motivation

Modeling of petroleum reservoirs and its application to pressure and production analysis have been studied for years, and can be generally classified as either numerical or analytical methods.

In reservoir engineering, there are only a few conventional methods for analytically solving the diffusivity equation for liquid flow. These include separation of variables, eigenfunction expansion, similarity transform, Laplace Transform, Fourier Transform, as well as Green's functions. Unfortunately, these solutions usually lend themselves only to geometrically symmetrical reservoir problems.

To overcome such problems, Lin[4], Caudle[5], Jankovic[6], and Haitjema[7] made use of superposition for approximate semi-analytical solutions in non-symmetrical scenarios (although these methods were generally limited to steady state applications for isobar and streamline mapping). Similarly, Guevara-Jordan[13] *et al* made use of this approach for streamline mapping of multiple wells in a sectionally homogeneous reservoir, while Britto[15] *et al* focused on type curve generation for a finite anomaly near a well within an infinite reservoir.

Acknowledging the popularity of finite-difference methods in petroleum engineering, the Green Element Method (GEM) and the Boundary Element Method (BEM) both have been studied extensively by Kikani[1], Archer[2], Pecher[3], and others. With increasing computational power, the GEM and BEM allowed for type curve generation during both transient and pseudosteady state (PSS) flow behavior in complex reservoir shapes – and in some cases time-dependent boundary conditions. Despite advantages over traditional analytical solutions, both GEM and BEM require programming capability for evaluating complex integrals and singular or ill-conditioned matrices (or at least access to numerical software libraries that did the calculations). It is documented that Sageev and Horne[49], who solved the problem of single well producing near a constant pressure or impermeable region in an infinite reservoir, encountered significant computational difficulties because of the complex nature of the solution. Similarly, Britto and Grader[50] who solved a similar problem had to deal with tedious

superposition procedures to ensure proper boundary conditions. These procedures become even more tedious, and computationally expensive during gas rate forecasting which is an iterative process (impractical for desk top calculators and excel code).

As a result, the objective of this paper is provide an approximate method for calculating pressure and rate profiles for multiple wells within an arbitrary shaped reservoir, solely using superposition methods without complex math or programming skills. The proposed method would maintain the appeal of GEM and BEM such as the reduction of the dimensionality of the problem by one (discretization of the boundary and not the domain), but eliminate the need for evaluating complex functions, and yet be far more versatile than simple geometric solutions.

Finally, by incorporating pressure and time transforms, the proposed solution would be suitable for accurate gas pressure-production forecasting in both conventional and CBM applications, during transient and boundary dominated flow regimes.

The Basic Process

Approximating Boundaries During Transient and PSS.

The theoretical justification of this work is based on superposition (a well known approach used in reservoir engineering applications), and is accurately described by Bear[8] who stated that any linear combination of solutions to a homogeneous linear partial differential equation (PDE) is also a solution to the that same PDE.

This statement means that if p_{D1} is a linear dimensionless solution for a single well in an infinite reservoir, then $C_1 \times p_{D1} + C_2 \times p_{D1} + .. C_n \times p_{D1}$ is also a solution where C_1, C_2 … C_n are arbitrary constants adjusted such that the combination is a new solution to the same liquid diffusivity equation, but subject to different boundary conditions.

In traditional applications for reservoir engineering, these solutions and their coefficients manifest themselves as image wells where the coefficients are known *a prior* since the spatial locations of image wells are chosen such that they are truly mirror images (both rate and location) of the real physical wells. Subsequently, it is well known that for multiple boundaries, there is a mirror effect between the image wells resulting in "images of image wells". As a result, without any consideration to varying rate schedule or multiple wells, generating a suitable solution for a single well in somewhat irregular shaped reservoir becomes a fairly tedious task due to calculating the large number of image wells (and their respective positions). In many instances, infinite summations of image wells are theoretically are required to ensure a stable solution. Earlougher[51] and Earlougher *et al*[10] present a comprehensive background on superposition and its application to the method of images concept.

In this work, a procedure is presented for approximating reservoir boundaries in complex geometries with less than a few dozen image wells and is adaptable for single phase oil, conventional gas and CBM reservoir modeling. The process in this work was inspired by Caudle[5], Jankovic[6], Lin[4], Leblanc[53], and others who used this approach for steady-state or PSS problems: images wells were arbitrarily placed and their coefficients (or rates) adjusted to achieve desired boundary conditions.

The flow rates of the pseudo image wells were determined such that an equal potential existed at a number of collocation or test points along the boundary. For practicality, these wells are called "pseudo" image wells as they are no longer true mirror images of any real physical well (or another image well). As a result, the solution process becomes a matrix problem as the rates at all pseudo image wells need to be determined simultaneously while evaluating the boundary conditions at test points. However, it is important to note the size of the matrix is reasonable compared to finite difference and finite element methods due the reduction in the dimensionality of the problem (no domain gridding is required). In other words, during the matrix operations, the normal potential is evaluated at a number of test points located along the boundary, and the image well rates calculated to ensure that difference was zero across the boundary. Appendix 1 describes the process for generating a dimensionless type curve for a single well within an arbitrarily shaped reservoir.

Haitjema[7] and Jankovic[6], who used a similar approach extensively in hydrology for steady-state applications, found that in a number of cases the errors between test points can become large and resulting in unacceptable solutions (increasing the number of test points only increased the error). The boundary condition is strictly enforced at the test points, but completely unrestricted at all other locations along the boundary. As a result, rather than meeting the desired boundary conditions exactly at the test points, an average solution was implemented by having more test points than pseudo image wells, resulting in a least squares solution where the boundary condition is met along the entire boundary in an average sense. Since the solution only honors the desired boundary condition at a number of test points along the boundary, the solution is approximate. If necessary, a singular value decomposition[13] approach was used to overcome ill-conditioned matrices.

Experimentation from the aforementioned authors has shown that 20 to 60 images wells with a 2:1 ratio of test points to pseudo image wells provided the best results[5,13,14], and that the average distance from the boundary to the bounding wells should be made equal to the average spacing of real wells. Based on less than a dozen tests, 36 pseudo image wells and 72 test points were used for all examples presented in this work. All pseudo image wells were placed approximately twice the average boundary distance from the center of the reservoir (refer to Figure 1). Once the type curve has been generated for each individual well in the real system, pressure profiles can be easily generated for each well in the system using conventional superposition assuming well rates are known.

Appendix 2 outlines the common calculation procedure for calculating the pressure response of multiple wells with varying (but known) rate history. For rate forecasting, the problem becomes a little more complex. Specifically, the

superposition algorithm presented in Appendix 3 must be re-arranged for the final time step in which the rates are unknown – however, since the rate of any well of interest is influenced by rate of all other wells in the system, a matrix problem occurs. Luckily, the matrix is always populated, and simple matrix operations can be utilized to solve for unknown rates.

Application & Testing

Numerical Validation & Testing

The reliability of "pseudo-image" programming was demonstrated by comparing this technique against analytical and finite difference simulation. Following an example presented by Archer[2], various solutions for a well is in a closed square reservoir with the well located at the center were evaluated (additional reservoir properties are shown in Table 1a). In this example, the reservoir fluid is single phase oil case.

In Archer's work, simulation runs were evaluated for a number of cells and gridding styles, with the number of cells ranging from 11x11 to 101x101 with both uniform and non-uniform gridding. Additionally, the same case was also evaluated using the Kappa non-linear simulator. The optimum results were obtained with the Kappa Voronoi gridding system and the pseudo-image well method as shown in Figure 2.

Following the work of Rattu[52], a type curve was generated with a numerical model using geometrically spaced grids for both areal and radial grids for a closed homogeneous reservoir. In this example, the accuracy of the numerical solution was improved by using equally spaced grids on a logarithmic basis (incidentally logarithmic timestep spacing was used in the simulation runs). Figure 3 shows good comparison between the pressure solutions obtained by the numerical and pseudo-image approach. For comparison, the analytical solution developed by Everdingen and Hurst[30] is also shown. Although not easily evaluated from Figure 3, a detailed review of the actual pressure data will show that even though the areal grid system can model the early time radial flow accurately, the radial grid system is preferred if highly accurate solutions are needed. Incidentally, as noted by Rattu, radial grids are less complex in construction and need less number of cells compared to the areal grids to give the same accurate solutions. The advantage of the pseudo-image well is that there is no need to consider the impact of gridding on early-time behavior as the method is not discretized within the domain. Also, once the number of test points has been specified, then the amount of computational effort is only proportional to the number of test points required to generate the desired geometry. In other words, the computational effort required to generate 8 sided polygon shaped reservoir may be the same as the computational effort to generate a square reservoir.

Note that in adapting the method for transient flow, pseudo image well superposition was used as inspired by Hong-Chen[14] who concluded that a single ring of pseudo image wells would bound the reservoir as long as superposition of the image well rates were taken into account in the solution process. Without the superposition effect of pseudo image wells, the solution was only sufficient for streamline generation.

Testing showed that the size of dimensionless time increment, Δt_D, should be in the range of 0.06 – 0.018, which is impractical for the typical time domains associated with PSS. Kikani[1] showed errors greater than 30% when using a dimensionless time, Δt_D, step greater than 0.025. For an error of 5% or less, a Δt_D step size of 0.005 or less was necessary, resulting in $2x10^6$ steps to generate late time solutions (which are generally in the order Δt_D = 10,000). The exponential growth in the number of rate changes required for rate superposition of pseudo image wells is memory intensive[1], and had to be continually repeated for each "real" well, before the various type curves could be superimposed to create a multiple well reservoir.

The problem becomes more complicated when adding pressure and time transforms during gas rate forecasting as the procedure becomes iterative. In order to alleviate the problem of computation speed, the solution process was adapted to Laplace Space as discussed in the next section of this paper.

Laplace Space Formulation of the Problem

In order to alleviate the problem of large computational calculations discussed in the previous section, the solution process was modified to operate predominately in Laplace space. The advantage that can be anticipated is that this maneuver removes the complication arising from rate superposition[1]. Another advantage (pointed out by Kikani[1] and Pecher[16]) is that since the solution at a given time is now no longer dependant on the solutions at previous times (no rate superposition in real time), there is no accumulation of computation errors for longer solution times. Ultimately, only space superposition needed to be considered in the overall solution process when generating the reservoir boundaries. For completeness, Appendix 4 shows the Laplace space Green's function for a cylindrical source in an infinite medium and the associated normal derivatives for the same function.

The only significant drawback of the Laplace transform technique is the need for an inversion method of the solution back to the real-time space. Originally, the solution process utilized the widely accepted Stefhest algorithm[18,17]. However, Stefhest's method suffered from some numerical instability problems for the solution when coded in Visual Basic, particularly at very early times.

An approach inspired by the work of Bourgeous[19], allowed for the easy inversion of Laplace solutions by simply using $p_D(t_D)=p_D(s)\times(s)$ where $s = 1/t_D$, and t_D is the time of interest. In his work, Bourgeois did not directly claim that this aforementioned calculation could be used to invert Laplace solutions. However, he did show that the Laplace and real space

asymptotes for the radial flow time period were nearly equivalent (assuming a vertical well, fully completed, in a homogeneous infinite-acting reservoir were nearly equivalent, refer to Appendix 5).

Figure 4 shows the inversion of the solution for a single well in closed reservoir using both Stefhest and the proposed non-numerical method inspired by Bourgeois. Although the results indicate that the solution is suitable for radial flow, the approximation is poor for dual porosity (assuming the classic Warren & Root[54] model). Figure 5 shows the Stefhest and Bourgeois approximation for a dual porosity scenario for an interporosity coefficient and storativity ratio of 1E-6 and 1E-1, respectively. Error is also evident when wellbore storage is included (as shown in Figure 6). Nonetheless, the results are adequate for PSS, the dominate flow regime in long-term deliverability forecasting. Similar approaches have been proposed by other authors using Laplace space transformations in coal bed methane applications, but were found not to be satisfactory for all time domains, particularly PSS. In most scenarios, the derivations of approximations were based on the assumption that the derivative of the function with respect to the natural logarithm approaches a straight line. These methods included Schapery's method[43], Najurieta's approximation[44], and what is commonly known as the complex inversion formula[17] . Figure 7 shows a comparison of some of methods evaluated in this work.

De-super Position for Wellbore Storage & Skin.

To add wellbore storage, skin, and dual porosity, a procedure generally termed "desuperposition" is utilized. Although by definition, the methodology is still superposition of linear solutions, it is called desuperposition in this paper to be consistent with the work presented by Gringarten, Ramey, and Raghavan[20], Chen and Brigham[21], Argawal[22], and Earlougher[23]. Although we could have used the approach introduced by Argawal, Al-Hussainy, and Ramey (1970), desuperpostion was simple to program.

Desuperposition is defined as modifying known p_D values to p_D's for different systems. The approach may be used for any drainage shape and well location. For example, to compute the pressure behavior, p_D, for a well located in the center of square with wellbore storage and skin, simply a) compute the pressure disturbance for the same system without wellbore storage ($c_D = 0$), b) remove (subtract) the solution for a single well in an infinite system (with zero wellbore storage or skin), and c) add the solution for well, including wellbore storage and skin, in an infinite system.

To show that desuperposition was a suitable approach, the wellbore pressure profile was generated analytically for a well located in the center of the radial composite system according to solution presented by Ambastha[41]. Using the solution using presented by Argarwal *et al*, wellbore skin and a positive skin were added in Laplace space, and then compared to a scenario in which wellbore storage and skin were added using desuperposition to a composite model originally generated with no wellbore storage or skin.

In both cases, the Laplace solutions were inverted to real space using Stefhest's algorithm. Figure 8 shows a comparison of the two solutions. Note, the values of C_D and "r_i" were chosen such that wellbore storage dominated a significant amount of the entire data set. These combinations of variables may unrealistic, but the example does illustrate that procedure is accurate and robust when compared to analytical procedures.

Influence of Anisotropy

An isotropic system can be transformed into an equivalent anisotropic using a transformation documented by Villegran[40], and others such as Earlougher[51]. Similarly, the transformation in this work (Appendix 6) ,is used to determine an equivalent isotropic reservoir dimensions for a given anisotropic medium. For the coal bed methane applications discussed later, the directional permeability is assumed to be associated with permeability in the fractures (or cleats), and not the permeability in matrix system.

In order to incorporate anisotropy, "x" and "y" coordinates were transformed as provided in (15), (16), and (17) in Appendix 6. Equation (15) represents the average permeability that will be used in dimensionless pressure conversions, and other calculations that require an average permeability input.

To evaluate the quality of the transformation, a test case was generated using the Kappa Voronoi simulator. Specifically, a circular reservoir was generated with a radius of approx. 3,000 ft., with k_x and k_y set to a ratio of 0.01. Figure 9 shows derivative and type curve for the transformed system as well as the explicit solution. Figure 10 shows a comparison of the original and transformed reservoir shapes.

Additional of Sectional Heterogeneity

So far, the solution is presented is only suitable for constant (anisotropic or isotropic), rock properties across the whole reservoir domain. This may not be practical since heterogeneities (shale lenses, structural features etc.) can occur abundantly in rock formations and may have a strong impact on the production pressure response. But there is a way to model large-scale heterogeneities and still apply the theory derived for a homogeneous medium. Specifically, the entire domain may be divided into several subdomains, or zones, representing regions of different but constant material properties.

In addition to the existing matrix calculations described in Appendix 1, an additional set of equations must be added. These equations represent the relations between pressure and normal fluxes in both zones at the common boundary points. Figure 11 shows the proposed matrix for a reservoir split into 2 permeability regions. The top section accounts for the pseudo-image well rates required ensuring reservoir boundary conditions in one region, while section 2 represents the pseudo-image wells required to bound the second region. Sections 3 and 4 represent pressure and flux continuity at the

interface. However, this approach is a significant deviation from similar problems in steady-state and PSS problems, and requires further evaluation for the theoretical justification. Conceptually, both reservoir regions would be independent and interact via the pseudo image well behavior along the interface of the two regions.

As a result, a simpler approach has been found to work reasonably well. Instead, the *Hawkins' equation*[46] (Appendix 7) is used to account for heterogeneity through a skin factor. Traditionally, Hawkins' equation has been used to approximate the permeability of an altered near wellbore zone, but is now used to account for sectional permeability variation within the subject reservoir.

In this work, the permeability of the region of which the well is situated is considered to be the altered zone, while the permeability of the area beyond the well region is considered to be representative of average reservoir. The radius of the altered zones is calculated based on area of the region of which the well of interest is situated. Following the work of Sagawa *et al*[49], it was found that the pressure performance well completed in a zone with a non-symmetrical high permeability streak could be reasonably approximated by an equivalent circular lens placed symmetrically around the wellbore. Specifically, after evaluating the performance of arbitrary well position in an irregularly shaped high permeability lens, it was found that in that at late times, all pressure curves became identical showing similar pseudo-radial flow with the same skin factor (refer to Figure 12).

As an example, a rectangular area with a permeability of 66.6 md was placed with a larger reservoir of 33.3 md (a ratio of 2). The area of the high permeability region is 155 Acres which equates to an effective radius of 1468 ft. Using Hawkins equation, this combination of parameters provides a wellbore skin of -6.37. Figure 13 shows a comparison of the dimensionless type curves for the explicit solution (using the Kappa Voronoi simulator) as well as the approximate solution. Although the early time transient solution is not honored, the overall rate-pressure drop relationship is honored during the PSS time period.

In a second example, the well and its high permeability region is moved towards the north west corner of the 33.3 md reservoir as shown in Figure 14. Also, the area of the 66.6 md region was slightly altered with an effective radius of 1932 ft. Using the Hawkins' equation, an effective wellbore skin of -4.4 was calculated. For the subject well, as shown in Figure 16, the long-term pressure/rate combination is honored.

In the final example, a multiple well system is created within a square reservoir and again a high permeability zone in the north west corner. The specified rate history of the well in the high permeability zone was varied from 10 to 1 and then 15 MMscf/d at 1 year increments. The second well located near the center of the reservoir had rates of 5, 8, and 4 MMscf/d also varied at 1 year increments. An anisotropy ratio of 3:1 for kx:ky also specified. In Figure 15, the pressure history for a) raw data for the well in the high permeability zone, b) a model incorporating the heterogeneity through skin, and c) a model without heterogeneity or the skin equivalent of -4.39. A review of the plot shows a reasonable history match and the suitability of the overall process for bounding reservoirs with anisotropy and section heterogeneity. Although not shown, if the production from the offset well is not included, the history match fails completely.

It surprising that Hawkins' equation produced reasonable results at the well of interest since according to the work of Furui *et al*[47], anisotropy can have a significant impact on the magnitude of the skin. Similar to transformation of the x-y coordinates of the reservoir shape in the previous examples, the effective radius results of the circular altered permeability zone is transformed into an ellipse (refer to Figure 10). Both Hawkin's and Furui's equations are provided in Appendix 7.

Using Furui's adaptation of the Hawkins' equation for above heterogeneity anisotropic reservoir, a skin factor of -4.22 was calculated – a slightly less improved situation than using the conventional Hawkins' relationship which predicted -4.39as mentioned above. Figure 15 show that both approaches produced similar results. Several hundred comparisons of Furui's and Hawkins equations for anisotropy ratios of 1 to 5; drainage radii ranging from 0.6 to 563 ft; average reservoir permeability for the unaltered region (greater reservoir) of 0.01 to 10 md; while the altered region (wellbore vicinity) was maintained at 18 md. Figure 16 shows a relatively linear skin relationship between the two methodologies. Nonetheless, more work is required in this area to ensure the proposed process is suitable for larger scale heterogeneity.

Gas Rate Forecasting

The concept of pseudo-time which handles variable viscosity and compressibility (μC_t) was, until recently, not amenable to a completely rigorous solution[24]. Rahaman[27] *et al*, introduced a new method for computing pseudo-time based upon material balance (Appendix 8) was primarily used for improving the forecasting of gas production when significant depletion was observed – gas properties are conceptually evaluated at average reservoir pressure during the life of the well. This is different from the pseudo-time introduced by Agarwal[28] in 1980 which focused on the pressure regime in wellbores and was used to correct the non-linear behavior of gas during buildups. Without introducing pseudo-time, gas rate forecasting using the traditional assumption of constant compressibility under-predicts the recoverable reserves (Figure 17). The pseudo-time formulation has corrected this problem and has significantly improved the quality of long-term forecasting of gas production.

The addition of pseudo-time to this paper does present some basic problems. Specifically, the pseudo-time formulation presented in Appendix 9 requires that one knows the gas rate at time "t" – this, of course, poses a problem when predicting or forecasting gas rates. As a result, the forecast solution becomes iterative. Specifically, the solution requires that the rate prediction initially be done with assuming normal or uncorrected time. The second iteration is then done using pseudo-time based on the previously calculated gas rates. Originally, convergence criteria on both gas rates and pseudo-time itself were incorporated in the solution process, however, extensive testing showed that five iterations are sufficient for most production

forecasts etc. For the work presented here, pseudo-time is based upon the total pool gas rate if multiple wells are producing in the reservoir. It has been noticed that the addition of pseudo-time to the problem moderately diminishes the speed of the solution process.

Addition of CBM.

To ensure that the process works for single CBM or shale gas, absorbed gas must be include in the material balance formulation. For this simulator, the material balance formulation of Clarkson and McGovern[45] is used as shown in Appendix 9. The form shown by Clarkson *et al* includes a term for average water saturation can change over time. However, for the purposes of this paper, it is assumed to equal S_{wi} at all times. In this example, data was generated using the Eclipse numerical simulator following the work of Clarkson *et al* (the data for the simulator runs are shown in the original Clarkson document). In this example, the coal is a dry coal such as those found in the Horseshoe canyon found in the Western Canadian Sedimentary Basin.

The results for the deliverability forecasts are shown in Figure 17. A review of this plot will show that the deliverability forecast based on the pseudo-image well method produced results comparable to the numerical model.

Multiwell Test

To show that the forecast technique works for multiple wells, a symmetrical case was developed. A 2x2 mile square reservoir with an OGIP of 35.4 Bcf was used. Four wells are placed symmetrical in the reservoir such that each well should be produce identical drawdown behavior if produced with identical gas rates. Additionally, the model results should compare very closely with a single well simulation configured with one-quarter of the drainage area. Type curve comparison with the KAPPA numerical simulator was performed as well [33,34,35,36]. For further verification, the analytical constant rate solution by Earlougher [10] *et al* for a single well located within the center of a rectangle was also generated – but for a square reservoir with ¼ of the size presented in Figure 19 (i.e. 8.85 Bcf), and with the well located centrally.

All four wells in the reservoir model produced at a constant rate of 5 MMscf/d for a period of 8766 hours (approximately one year), producing a total of 7.31 Bcf. Sandface pressures were calculated at 100 logarithmically spaced points.

All four wells in the reservoir model calculated nearly identical sandface pressures. Figure 21 shows the "Single-Well" model was very similar to any well from the original pressure forecast, with a slight difference of 13 psi (0.3% of initial reservoir pressure). This suggests that a no-flow boundary is forming half-way between each well, isolating each well into an identical one-square-mile drainage area as shown in Figure 21. Figure 22 shows the dimensionless pressure derivative for one of the 4 test wells along with a single well profile for a ¼ reservoir.

General Solution Process

Given the theory outlined in the previous sections, the rate pressure profile for multiple wells in an arbitrary shaped reservoir can be generated according to the following process.

1) Generate individual type curves for the "real" well:
    a. Using the Laplace Space formulation of the problem, solve for the pseudo image well rates by solving the matrix calculations as described in Appendix 1.
    b. Repeat (a) for each time t_D to generate a type curve that starts at transient and ends at pseudo steady-state.
    c. Repeat (a) for each observation point with the reservoir (corresponding to remaining real well locations).
    d. Convert the type curve to the real space formulation of the problem using $p_D(t_D)=p_D(s)\times(s)$ where $s = 1/t_D$.
    e. Use De-superposition to add wellbore storage, dual porosity, skin, etc. to the existing type curves.
    f. When evaluating wellbore pressure for known rates, generate:
        i. Generate pseudo-time for the given rate history, and a pseudo-pressure table from known fluid properties.
        ii. Convert pseudo-time from (i) to dimensionless time (t_{Da}), and lookup dimensionless pressure (p_D) from (d) above.
        iii. Using pseudo-pressure table, convert dimensionless pressure (p_D) to pseudo-pressure, and then convert pseudo-pressure to real wellbore pressures (p_{wf}).
2) Generate multi-rate responses for individual or multiwell reservoirs
    a. If rate forecasting, skip (2) and proceed to (3).
    b. After performing (1) above, use conventional superposition as described in Appendix 2 for generating single or multi-rate responses.
3) Use conventional superposition-in-time to generate multi-rate scenarios for each well.
    a. When evaluating rates for known wellbore pressure history, generate:
        i. Generate pseudo-pressure table from known fluid properties.
        ii. Convert pseudo-pressures to dimensionless pressure (p_D), and back calculate rate "q" for desired dimensionless real time (t_D) according to Appendix 3.
        iii. Calculate new pseudo-time t_{Da} based on q, and repeat procedure until q and t_{Da} convergence.

Conclusions & Further Work

The following conclusions and recommendations were observed:

a) A single ring of pseudo-image wells can be used to generate no-flow boundaries for arbitrary shaped reservoirs, with multiple wells. Anisotropy can be easily incorporated into the process through coordinate transformation. Also, sectional heterogeneity can be incorporated into the process using a skin equivalent (although further work is required to evaluate approximation for multiple permeability sections etc.)
b) The methodology presented appears to be suitable for long-term pressure and production forecasting, using pseudo-time and pseudo-pressure transformations. The procedure can also be adapted for single phase CBM (or similar) by incorporating the appropriate material balance and pseudo-time modifications.
c) Anisotropy (directional permeability) can be easily incorporated into the solution using simple transforms
d) There is room for additional research into adapting the method for multiphase flow.

Nomenclature

A	Reservoir Area (ft^2)
B_g	Gas FVF (Dim)
B_{gi}	Gas FVF at Initial Conditions (Dim)
C_A	Shape Factor, Dimensionless
C_n	Constant at Position/Index "n"
c_t	Total System Compressibility ($psia^{-1}$)
c_{ti}	Total System Compressibility at P_i ($psia^{-1}$)
h	Net pay (ft)
K0	Bessel Function
K1	Bessel Function
OGIP	Original-Gas-In-Place (scf)
$m(p)$	Pseudo-pressure of "P" ($psia^2/cp$)
$m(p_i)$	Pseudo-pressure of "P_i" ($psia^2/cp$)
$\Delta m(p)$	Change in Pseudo-pressure
m(p)'	Derivative of pseudo-pressure w/r ln(t)
n	Index
P	Pressure (Psia)
P_i	Initial Reservoir Pressure (psia)
P_{wf}	Flowing Sandface Pressure (psia)
p_D	Dimensionless Pressure
p_D'	Dimensionless Pressure Derivative w/r $\ln(t_D)$
$p_D(s)$	Dimensionless Pressure in Laplace Space
q_g	Gas Rate at Standard Conditions (MMscf/d)
Q_g	Cumulative Gas Produced (MMscf)
s'	Wellbore Skin
s	Laplace Variable
S_{wi}	Initial Water Saturation (fraction)
t	Time (hrs)
t_a	Pseudo-time (hrs)
t_D	Dimensionless Time referenced to r_w
t_{Da}	Dimensionless Pseudo-Time referenced to r_w
t_{DA}	Dimensionless Time referenced to Area (A)
k	Permeability (md)
r_w	Wellbore radius (ft)
r_{wa}	Apparent Wellbore Radius (ft)
r_D	Dimensionless radius (Dim).
T_f	Formation Temperature (oR)
x_D	Dimensionless X-Coordinate of Well
y_D	Dimensionless Y-Coordinate of Well
x_{Do}	Dimensionless X-Coordinate of Observation Point
y_{Do}	Dimensionless Y-Coordinate of Observation Point
γ	Euler's Constant
γ_m	Permeability Modulus
ϕ	Porosity
μ_g	Gas viscosity (cp)
μ_{gi}	Gas viscosity at P_i (cp)

σ Stress
z_{wf} Real gas deviation factor evaluated wellbore pressure (Dim)
z_i Real gas deviation factor evaluated at initial reservoir pressure (Dim)

Subscripts:

a Pseudo-time
A Area
D Dimensionless
g Gas
i Initial
PSS Pseudo-steady state
t Total
wf Wellbore Flowing
w Wellbore
m Modulus

References

1. Kikani, J. "Application of Boundary Element Method to Streamline Generation and Pressure Transient Testing", Ph.D. Thesis, Stanford University, 1989.

2. Archer, R.A.: "Computing Flow in Pressure Transients in Heterogeneous Media Using Boundary Element Methods", Ph. D Thesis, Stanford University, March 2000.

3. Pecher, R., "Boundary Element Simulation of Petroleum Reservoirs with Hydraulically Fractured Wells", Ph. Thesis, University of Calgary, 1999.

4. LIN, JER-KAUN "An Image Well Method for Bounding Arbitrary Reservoir Shapes in the Streamline Model"

5. Caudle, b.h., "Mechanics of Fluids in Permeable Media", Course Notes, University of Texas at Austin, 1996.

6. Jankovic, I., "High-Order Analytic Elements in Modeling Groundwater Flow", Ph.D Thesis, University of Minnesota, 1997.
7. HAITJEMA , "Analytical Modeling of Groundwater flow Flow", Academic Press, New York, 1995.

8. Bear, J., "Dynamics of Fluids in Porous Media", Dover Publications Inc., New York, 1972

9. Matthews, C.S., and Russell, D.G.: "Pressure Buildup and Flow Tests in Wells", SPE Monograph 1, 1967.

10. Earlougher, R.C., Jr., Ramey, H.J., Miller, F.G., and Meuller, T.D., :"Pressure Distributions in Rectangular Reservoirs", J. Pet. Tech., February 1968, 199-208; Trans., AIME, 243.

11. "Gas Well Testing", 3rd Edition, ERCB Publication.

12. "Gas Well Testing: Theory & Practice", 4th Ed. Metric. Alberta Energy & Utilities Board Publication.

13. Guevara-Jordan, J.M., Rodriquez-Hernadez,: "Applications of Singular Value Decomposition to Determine Streamline Distribution for Sectionally Homogeneous Reservoirs", SPE International Symposium on Oil Field Chemistry, Texas, 19-16 February 2001. SPE Paper No. 65414

14. Hong-Chen, L.: "A Method for Bounding Irregularly-Shaped Reservoir Subject to Unsteady State Flow", Ph.D. Thesis, University of Texas at Austin, 1975.

15. Britto, P., and Sageev, A., "The Effects of Size, Shape, and Orientation of an Impermeable Region on Transient Pressure Testing", SPE California Regional Meeting, Ventura, April 8-10, 1987. SPE Paper No. 16376.

16. Pecher, R., and Stanislav, J. F.: "Boundary Element Techniques in Petroleum Reservoir Simulation", Journal of Petroleum Science and Engineering, 17, 1997, 353-366.

17. Cox., D "Solution of Unsteady Flow Problems in Porous Media", PE 5980, Course Notes, Colorado School of Mines.

18. Stefhest, H.: "Numerical Inversion of Laplace Transforms", Communication of the ACM, Jan. 1970, Vol. 13, No. 1. 47-49.

19. Bourgeois, M., "Well Test Interpretation Using Laplace Space Typecurves", Elf Aquitaine, April 1992.

20. Gringarten, A, C., Ramey, H.J., Jr., and Raghavan, R., "Unsteady-State Pressure Distributions Created by a Well With a Single Infinite-Conductivity Vertical Fracture" Soc. Pet. Eng. J. (Aug. 1974) 347-360; Trans., AIME, 257.

21. CHEN, JSIU-KUO & BINGHAM, W.E., "Pressure Buildup for a Well With Storage and Skin in a Closed Square", SPE-AIME, 44th Annual California Regional Meeting, SPE Paper No. 4890, April 4-5, 1974.

22. ARGAWAL, R.G., "A new Method to Account For Producing Time Effects When Drawdown Type Curves Are Used to Analyze Pressure Buildup and Other Test Data"

23. MATTHEWS,C.S., and RUSSELL, D.G.,"Pressure Buildup and Flow Tests in Wells", SPE Monograph 1, 1967.

24. Blasingame, T.A., and Lee., W.J. "The Variable-Rate Reservoir Limits Testing of Gas Wells" SPE 17708, 1988 SPE Gas Technology Symposium.

25. Mattar, L., "Tech Talk: Pseudo-Time or Pseudo-Pressure?", Fekete Assoc. News Letter, Winter 2001.

26. AL-HUSSAINY, R, and Ramey, H.J., Jr. "Application of Real Gas Flow Theory to Well Testing and Deliverability Forecasting", JPT (196) 18, 624-636.

27. Raghavan, R. "Well Test Analysis", 1993 Prentice Hall.

28. Rahaman, A., Mattar, L., and ZAORAL, K., "A New Method for Computing Pseudo-Time for Real Gas Flow Using the Material Balance Equation", CIPC Annual Conference, Calgary, June 8-10, CIM Paper No 2004-182.

29. AGARWAL, R.G., "Real Gas Pseudo-time – A New Function for Pressure Buildup Analysis of MHF Gas Wells", SPE Annual ATCE , Las Vegas, Sept 23 -26. SPE Paper No. 8279.

30. van EVERDINGEN, A.F., & HURST, W., "Application of the Laplace Transformation to Flow Problems in Reservoirs", *Trans*, AIME (1949), 186, 305-24.

31. Matthews, C.S., Brons, F., and Hazebroek, P., "A Method for Determination of Average Reservoir Pressure in a Bounded Reservoir", Trans., *AIME* **201** (1954) 182-191.

32. Agarwal, R.A., Garnder, D.C, AND Kleinsteiber, S.W, "Analyzing Well Production Dada Using Combined-Type-Curve and Decline Curve Analysis Concepts", SPE 57916, 1988 SPE Annual Technical Conference and Exhibition, New Orleans, Louisiana

33. Ibhrahim, M., Wattenbarger, R.A, AND W. Helmy "Determination of OGIP for Tight Gas Wells – New Methods", CIM 2003-012, CIPC 2003, Calgary, Alberta.

34. Z. E. Heinemann and C.W. Brand, Modeling Reservoir Geometry with Irregular Grids, paper SPE 18412 presented at 10th SPE Symposium on Reservoir Simulation, Houston, 1989.

35. C. Palagi, Generation and Application of Voronoi Grid to Model Flow in Heterogeneous Reservoirs, Ph. D., Thesis of Stanford University, 1992.

36. C. Palagi and K. Aziz, The Modeling of Vertical and Horizontal Wells with Voronoi Grid, paper SPE 24072 presented at the SPE Western Regional Meeting, Bakersfield, 1992.

37. S. Verma, Flexible Grids for Reservoir Simulation, Phd Thesis of Stanford University, 1996

38. Bourgeouis, M. "Well Test Interpretation Using Laplace Space Typecurves", April 1992, SUPRI-D Publication, Stanford University.

39. Gardner, D.C., Hager, C.J., and Argarwal, R.G., "Incorporating Rate-Time Superposition into Decline Type Curve Analysis", SPE Paper No. 62475 prepared for presentation at the 2000 SPE Rocky Mountain Regional Meeting/ Low Permeability Reservoirs Symposium, Denver, 12-15 March.

40. Villegran, J. A. A.: "Analysis of Long-Term Behavior in Tight Gas Reservoir: Case Histories", Ph.D., Disseratation, Texas A&M University, College Station (2001).

41. Ambastha, A.K.: "Pressure Transient Analysis for Composite Systems", Ph.D. Dissertation, Stanford University, Stanford (1988).

42. Anbarci, K., and Ertekin, T.,: "A Comprehensive Study of Pressure Transient Analysis with Sorption Phenomena for Single-Phase Gas Flow in Coal Seams", SPE Paper No. 20568 presented at 65th Annual Technical Conference, New Orleans, 1990.
43. Schapery, R.A.: : "Approximate Methods of Transform Inversion for Viscoelastic Stress Analyis", paper presented at the Fourth U.S. National Congress of Applied Mechanics (1961), p. 1075-1085

44. Najurieta, H.L.,: "A Theory fore Pressure Transient Analysis in Naturally Fractured Reservoirs", JPT, (July, 1980), p. 1241-1250.

45. Clarkson, C. R., and McGovern, J.M.: "A New Tool for Unconventional Reservoir Exploration and Development Applications"

46. Hawkins, M. F.: "A Note on the Skin Effect", paper SPE 732-G, JPT, 1956 December.

47. Furui, K., Zhu, D., and Hill, A.D.: "A Rigorous Formation Damage Skin Factor and Reservoir Inflow Model for a Horizontal Well", paper SPE 84964 presented at the 2002 International Symposium and Exhibition on Formation Damage Control, Louisiana, 17 December, 2002.

48. Sagawa, A., Corbett, P. W. M., and Davies, D.R.: "Pressure Transient Analysis of Reservoirs with a High Permeability Lens Intersected by the Wellbore", Journal of Petroleum Science and Engineering, February 27 (2000).

49. Sageev, A., and Horne, R.N.: "Pressure Transient Analysis in a Reservoir with a Compressible or Impermeable Circular Subregion: Gas Cap or EOR-Induced", paper SPE 12076 presented at the 1983 SPE Annual Technical Conference and Exhibition, San Francisco, Sept 5-9.

50. Britto, P.R., and Grader, A.S.: "The Effects of Size, Shape, and Orientation of an Impermeable Region on Transient Pressure Testing," SPEFE (Sept 1988) 585-606.

51. Earlougher, R.C.: "Advances in Well Test Analysis" SPE Monograph #5, 1997. SPE New York.

52. Rattu, B. C.: "Modeling Techniques for Simulating Well Behavior" M.Sc. Thesis, Texas A&M, May 2002.

53. LeBlanc, J. L.: "A Streamline Model For Secondary Recovery" paper SPE 2865 presented at the 1970 Ninth Biennial Production Technique Symposium, Wichita Falls, 14-15 May.

54. Warren, J. E., and Root, R. J.: "The Behavior of Naturally Fractured Reservoirs" paper SPE 426 presented at the Fall Meeting of the1962 Society of Petroleum Engineers, Los Angeles, 7-10 Oct.

Appendix 1 – Superposition and Single Well Type Curve Generation

The principle of superposition means the presence of one boundary condition does not affect the response produced by the presence of other boundary or initial conditions, and that there are no interactions among the responses produced by the different boundary conditions.

The fact that most continuity equations developed in fluid flow in porous media applications are linear, permits the use of a powerful tool – the principle of superposition – in solving them with or mixed, inhomogenous (linear) boundary conditions[8]. Briefly, the principle of superposition states that if p_{D1} and p_{D2} are two particular solutions of a, homogeneous linear partial differential equation, then p_{D1} and p_{D2} are also particular solutions (1) where C_1 and C_2 are constants that satisfy the new desirec boundary conditions.

$$p_D = C_1(p_{D1}) + C_1(p_{D2}) \tag{1}$$

In typical reservoir engineering applications, (1) can be expressed in a general case as show in (2), where again the constants are adjusted so that the "new" boundary conditions are satisfied. In certain cases, the summation in (2) may need to be extended to infinity in order to satisfy the desired boundary conditions. Note, (2) is expressed in dimensionless for according to definitions in Appendix 10.

$$p_D = \sum_{i=1}^{n} C_n(p_{Dn}) \tag{2}$$

In order to ensure a no-flow boundary condition, (2) must be evaluated such that $dp_D/d\mathbf{n} = 0$ along the proposed boundary. Note, the impact all pseudo image wells and the real well must be taken into account. If one considers all real and pseudo-image wells, the normal derivative at any point on the boundary can be written as (3) shown below, where x_{Do} and y_{Do} represent observation points on the boundary. The angle (α) is the boundary angle and is measured from the positive horizontal axis to the normal line. If C_n is adjusted such that (7) is zero at all test points, then a suitable boundary condition has been met. Equation (3) is the Laplace formulation of the problem.

$$\left.\frac{\partial[p(y_D, x_D, s)_D]}{\partial n}\right|_{Real} = \sum_{n=1}^{N} C_n\left[\left[\cos(\alpha)\frac{\partial[p(x_{Do}, s)_D]}{\partial x_{Do}} + \sin(\alpha)\frac{\partial[p(y_{Do}, s)_D]}{\partial y_{Do}}\right]\right] \tag{3}$$

In solving (3) for C_n, an M x N results, where N represents the number of image wells, and M represents the number of test points along the desired reservoir boundary. If there are more test points than pseudo image wells, the solution is met in an average sense and can be solved using least squares reduction or other matrix solution processes. If M = N, the solution is met exactly at the test points with little or no control at boundary positions in between the test points. The procedure is then repeated for each additional real well in the system. Once type curves are generated for each real well, they are inverted to real space.

Appendix 2: Pressure Forecasting (Single or Multi Well Systems)

Once type curves have been generated for each well in the system, pressure profiles for multiple wells with a varying rate can easily be generated using conventional superposition methods as shown in (4). The integer "Nt" represents the current time step; "ti" represents the previous time steps; "R" represents the well of interest; and finally "NR" represents the total number of real wells in the system. Note (12) is based upon pseudo-time (Appendix 7) for gas systems, but can be replaced with conventional time for linear fluid systems.

$$p(t_{D,Nt})_{D_R} = \sum_{R=1}^{NR}\sum_{ti=1}^{Nt}\left(\Delta q_{R,t}\cdot p_D(t_{Da_{NT}} - t_{Da_{ti-1}})\right) \tag{4}$$

Appendix 3: Production / Rate Forecasting

Once type curves have been generated for each well in the system, production profiles can be generated for each well with varying specified line pressure. However, the procedure is somewhat more complicated than generating pressure profiles at outlined in Appendix 2. Although a number of convolution and deconvolution methods were reviewed, the most effective method was found to be "back-calculating" the necessary rate at a specified time to meet the desired back pressure. As an example, (5) shows the matrix formulation for the general real well case where a different backpressure has been specified for each well. Generally speaking (5) is just a re-arrangement of (4) for the last unknown rate in the rate schedule. A matrix solution is required as we want to determine the rates of each well while incorporating the influence of the offset wells. The unknown rates $\Delta g_{g,n}$ can be solved using $x = A^{-1}b$ where A represents the desired backpressure at each well and b represents previous production.

(5)

$$x = \begin{vmatrix} \Delta q_{@1} \\ \Delta q_{@1} \\ \cdots \\ \Delta q_{@NR} \end{vmatrix} = \begin{vmatrix} p_{D,1@1}(\Delta t_D) & p_{D,2@1}(\Delta t_D) & p_{D,1NR@1}(\Delta t_D) \\ p_{D,1@2}(\Delta t_D) & p_{D,2@2}(\Delta t_D) \cdots & p_{D,NR@2}(\Delta t_D) \\ & \cdots\cdots & \\ p_{D,1@NR}(\Delta t_D) & p_{D,2@NR}(\Delta t_D) & p_{D,NR@NR}(\Delta t_D) \end{vmatrix}^{-1} \begin{vmatrix} p_{D,spec} - \sum_{R=1}^{NR}\sum_{ti=1}^{Nt-1}\left(\Delta q_{R,t}\cdot p_D(t_{Da_{NT}} - t_{Da_{ti-1}})\right) \\ p_{D,spec} - \sum_{R=1}^{NR}\sum_{ti=1}^{Nt-1}\left(\Delta q_{R,t}\cdot p_D(t_{Da_{NT}} - t_{Da_{ti-1}})\right) \\ \cdots \\ p_{D,spec} - \sum_{R=1}^{NR}\sum_{ti=1}^{Nt-1}\left(\Delta q_{R,t}\cdot p_D(t_{Da_{NT}} - t_{Da_{ti-1}})\right) \end{vmatrix}$$

Appendix 4: Green's Functions (Laplace Space Solutions)

The appropriate Laplace space Green's function[3,26] for a cylindrical source is shown in (6) and assumes an unbounded infinite reservoir. In order to ensure the desired boundary condition (i.e. a no-flow boundary), the pressure gradient normal to the boundary must be equal to zero.

$$p_D(s) = \frac{K_0(r_D\sqrt{s})}{s^{3/2}K_1(\sqrt{s})} \tag{6}$$

The derivatives of (6) with respect to x_D and y_D at an arbitrary location (i.e. an observation point on the reservoir boundary) are shown in (7) and (8). The normal derivative at some test point on boundary is given by (6). The derivation of (7) to (8) can be found in Hong-Chen[14], and other sources. Note, $r_D = (\Delta x_D^2 + \Delta y_D^2)^{1/2}$, while $\Delta x_D^2 = (x_{Do}-x_{Dw})^2$ and while $y_D^2 = (y_{Do}-y_{Dw})^2$

$$\frac{\partial[p(r_D,s)_D]}{\partial x_D} = -\frac{1}{2}\left[\frac{K_1(r_D\sqrt{s})}{r_D s}\right]\frac{2(\Delta x_D)}{K_1(\sqrt{s})} \tag{7}$$

$$\frac{\partial[p(r_D,s)_D]}{\partial y_D} = -\frac{1}{2}\left[\frac{K_1(r_D\sqrt{s})}{r_D s}\right]\frac{2(\Delta y_D)}{K_1(\sqrt{s})} \tag{8}$$

$$\frac{\partial[p(y_D,x_D,s)_D]}{\partial n} = \cos(\alpha)\frac{\partial[p(r_D,s)_D]}{\partial x_{Do}} + \sin(\alpha)\frac{\partial[p(r_D,s)_D]}{\partial y_{Do}} \tag{9}$$

Appendix 5: Semi-Log Behavior

Bourgeois[19,37] showed that if one considers a vertical fully penetrating well in a homogeneous infinite-acting reservoir, then the asymptote for real space solution in (10) is graphically equivalent to the asymptotic Laplace space solution in (11). Specifically, plots of p_D (t_D) vs. t_D and $s\bar{p}_D(s)$ vs. 1/s have the same asymptote behavior which is the well-known semi-log straight line. The plots in real space and Laplace space are not exactly the same, but its does imply that pD(s) can be converted to real space by simply multiply by $s = 1/t_D$ for a given $t_D = 1/s$ as summarized in (12). Similarly, Schapery[43] showed that if radial flow exists, then the inverse of the Laplace transformation can be approximated by (13). Later, Najurieta[44] introduced an improved Schapery technique which materializes in the form of (14).

$$p_D(t_D) = \frac{1}{2}(\ln(t_D) + 2\ln(2) - \gamma) \tag{10}$$

$$s\widetilde{P}(s)_D = \frac{1}{2}(\ln(\tfrac{1}{s}) + 2\ln(2) - 2\gamma) \tag{11}$$

$$p_D(t_D) = s \cdot f(s)_{s=\frac{1}{t_D}} \tag{12}$$

$$p_D(t_D) = s \cdot f(s)_{s=\frac{0.5}{t_D}} \tag{13}$$

$$p_D(t_D)_D = s \cdot f(s)_{s=\frac{1}{\gamma t_D}} \tag{14}$$

Appendix 6: Anisotropic Reservoirs

The following equations are used to calculate an equivalent isotropic reservoir from an anisotropic reservoir. Absolute permeability is calculated using (15), where k_x and k_y represent permeability in the x and y-directions respectively, and are considered to be the principal permeabilities[51]. The specified dimensions in the x and y-direction are transformed into new dimensions using (16) and (17). The solution process remains constant when expressed in the new coordinate system. However, permeability as defined by (15) must be used in replace of k in all dimensionless time and pressure definitions etc.

$$\bar{k} = (k_x k_y)^{0.5} \tag{15}$$

$$x_{new} = x_{old}(\bar{k}/k_x)^{0.5} \tag{16}$$

$$y_{new} = y_{old}(\bar{k}/k_y)^{0.5} \tag{17}$$

Appendix 7: Sectional Permeability

Sectional permeability is incorporated into the solution process using the well known Hawkin's[46] formula shown in (18), where k_a and r_a represent the permeability and radius of permeability section within the well vicinity. The radius r_a is calculated from the area of the permeability section assuming a circular drainage region as defined in (19). For anisotropic reservoirs, Furui *et al*[47] presented an equation for calculating skin factor as shown in (21), where r_{dH} represents the "long" direction along the transformed ellipse. For this paper, k_x is defined as the maximum principle permeability.

$$S = \left(\frac{\bar{k}}{k_a} - 1\right) \ln\left[\frac{r_a}{r_w}\right] \tag{18}$$

$$r_a = \left[\frac{Area}{\pi}\right]^{0.5} \tag{19}$$

$$s = \left[\frac{\bar{k}}{k_d} - 1\right] \ln\left[\frac{1}{I_{anis}+1}\left(\frac{r_{dH}}{r_w} + \sqrt{\frac{r_{dH}^{\ 2}}{r_w^{\ 2}} + I_{anis}^{\ 2} - 1}\right)\right] \tag{21}$$

Appendix 8: Pseudo-Time and Pseudo-Pressure

For long-term multi-well drawdown in bounded reservoirs, the formulation of pseudo-time based upon material balance is given below in (22). As can be seen, the pseudo-time calculation requires that average reservoir pressure be determined which makes the rate prediction process in Appendix 8 iterative. Gas rates and average reservoir pressure are based on total pool production. If all wells are shut-in, then the pseudo-time calculation reverts to numerical evaluation. Note, pseudo-time is typically denoted by a subscript "a". For (22) to be used with a CBM gas simulator, it must account for the desorption compressibility of the coal or shale, which is defined by (26). However, a simple approximation can be accomplished (and the original solution process unaltered) by using a proxy permeability in the dimensionless time definition as defined by (27) and (28).

$$t_a(t) = (u_g c_t)_i \int_0^t \frac{\partial t}{u(\overline{P_R})c_t(\overline{P_R})} = \frac{GZ_i}{2P_i S_{gi}}\left[\frac{\overline{\Delta mp}_{01}}{q_{gt1}} + \frac{\overline{\Delta mp}_{12}}{q_{gt1}} + ... \frac{\overline{\Delta mp}_{n-1,n}}{q_{gtn}}\right] \tag{22}$$

$$c_d = \frac{B_g \rho_c V_L P_L}{32.0368(P_L + P_R)^2 \phi} \tag{26}$$

$$k' = \frac{k \bullet h'}{real} \tag{27}$$

$$h' = \frac{OGIP_{free+abs}}{Area\phi(1 - S_{wi})} \tag{28}$$

Pseudo-pressure is commonly used in well test analysis of gas reservoirs [23,24,26,27,28]. The formulation used in this work is presented in (29).

$$mp(p) = \frac{1}{2}\int_{pref}^{P} \frac{p}{u(p_{wf})z(p_{wf})}\partial p \tag{29}$$

Appendix 9: Absorbed Gas Material Balance

Equation (30) was first presented by Clarkson & McGovern[45] in a previous paper. However, it is important to note that it incorporates the free-gas storage in the macrpores (fractures + matrix) as well as the absorbed component.

$$\frac{P}{P + P_L} + \frac{32053\phi(1 - \bar{S}_w)}{V_L B_g \rho_c} = \frac{-0.7538}{V_L A h \rho_c} G_p + \left[\frac{P_i}{P_i + P_L} + \frac{32053\phi(1 - \bar{S}_w)}{V_L B_{gi} \rho_c}\right] \tag{30}$$

Appendix 9: Pseudo-Steady State and Reserve Analysis

For long term production at a constant rate, (31) can be used to represent pseudo-steady state flow in dimensionless terms[23,24,25,26,27,28]. The Bourdet derivative associated with this equation is shown in (32). When appropriate, (31) and (32) were used to evaluate the PSS of the pseudo image well approach.

$$p_D(t_D) = \frac{2t_D}{r_{eD}^{\ 2}} + \ln(r_{eD}) - \frac{3}{4} \tag{31}$$

$$\frac{\partial p_D(t_D)}{\partial(\ln(t_D))} = \frac{2t_D}{r_{eD}^{\ 2}} \tag{32}$$

Appendix 10: Dimensionless Variable Definitions

The following definitions for dimensionless variables are used throughout this paper.

$$p_D = \frac{kh\left(m(p_i) - m(p_{wf})\right)}{1.417 \cdot 10^6 T_f q_g} \tag{33}$$

$$\overline{p_D} = \frac{kh\left(m(p_i) - m(p_R)\right)}{1.417 \cdot 10^6 T_f q_g} \tag{34}$$

$$t_{AD} = \frac{0.0002637kt}{(\phi\mu_g c_t)A} \tag{35}$$

$$t_{Da} = \frac{0.0002637k't_a}{(\phi\mu_g c_t)r_w^{\ 2}} \tag{36}$$

$$t_D = \frac{0.0002637kt}{(\phi\mu_g c_t)r_w^{\ 2}} \tag{37}$$

$$t_{Da} = \frac{0.0002637kt_a}{(\phi\mu_g c_t)r_w^{\ 2}} \tag{38}$$

Figure 1. Location of Control Points and Image Wells (ft)

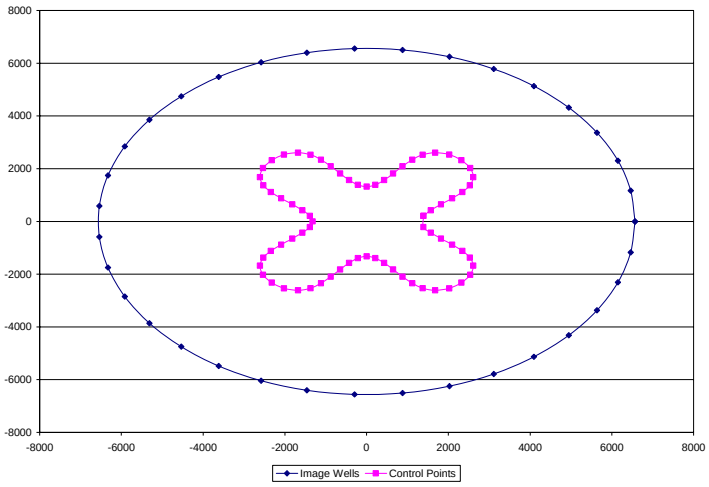

Figure 2. Numerical Validation Example (Archer)

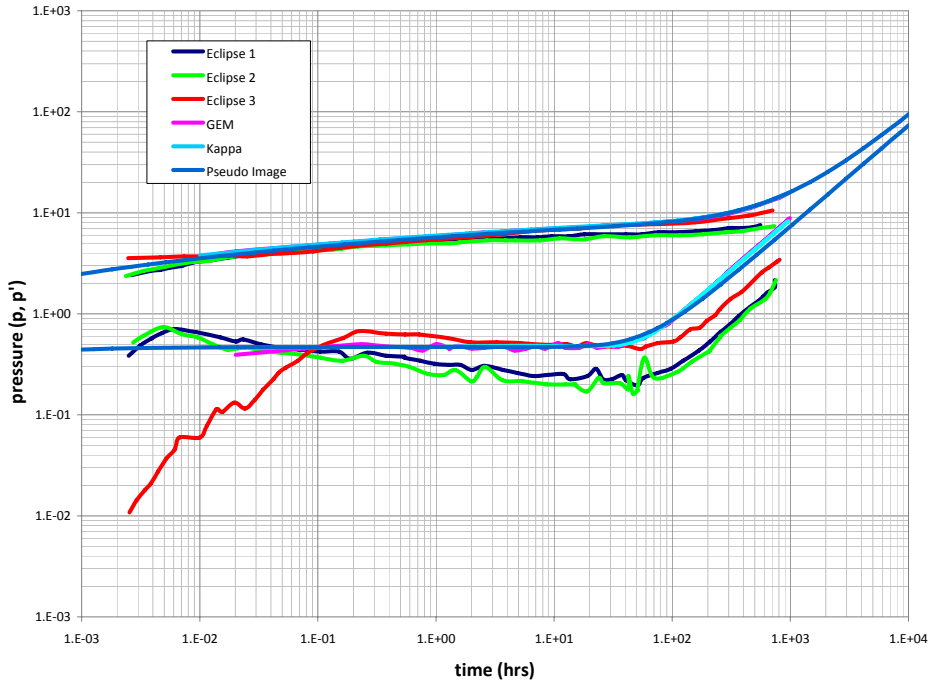

Figure 3: Numerical Validation Example (Rattu)

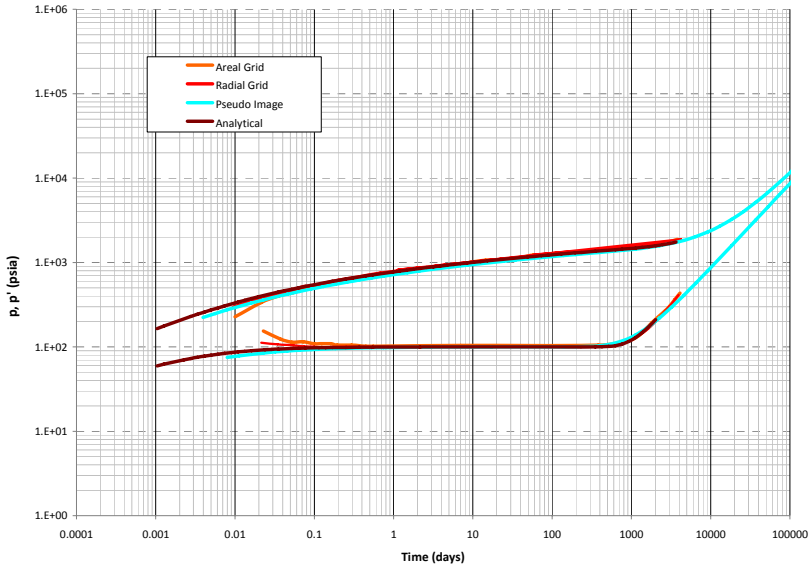

Figure 4. Stefest vs. Approximate Solution for Homogeneous Reservoir

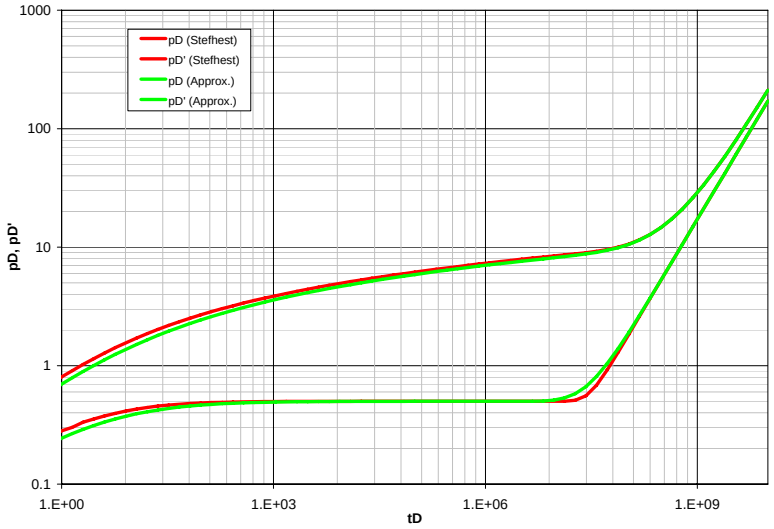

Figure 5. Stefhest vs. Bourgeois for Dual Porosity

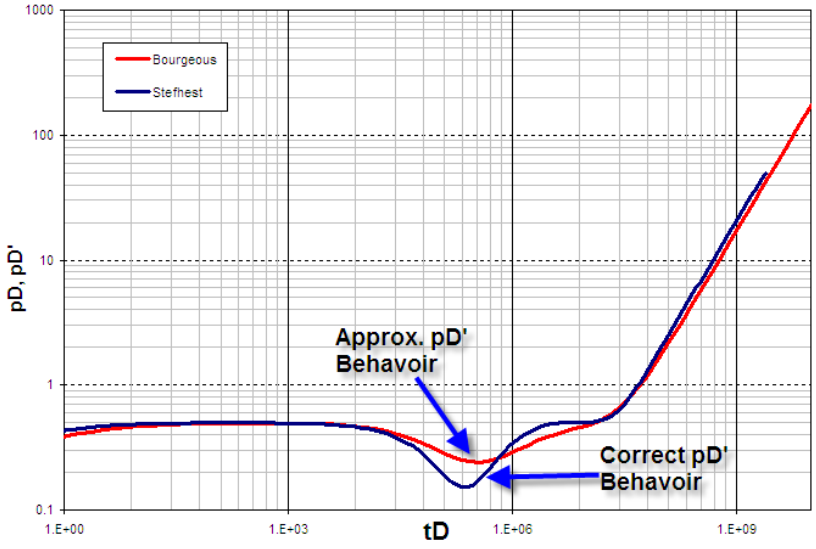

Figure 6. Stefhest vs. Bourgeois for Wellbore Storage

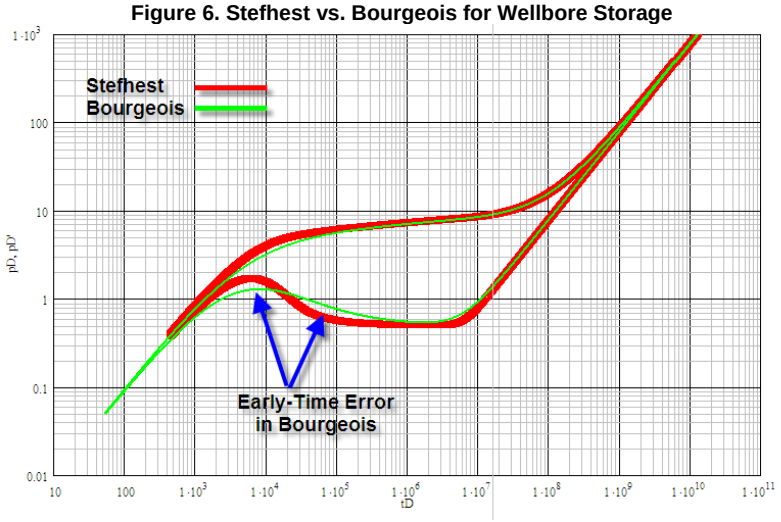

Figure 7. Stefhest vs. Other Approximations

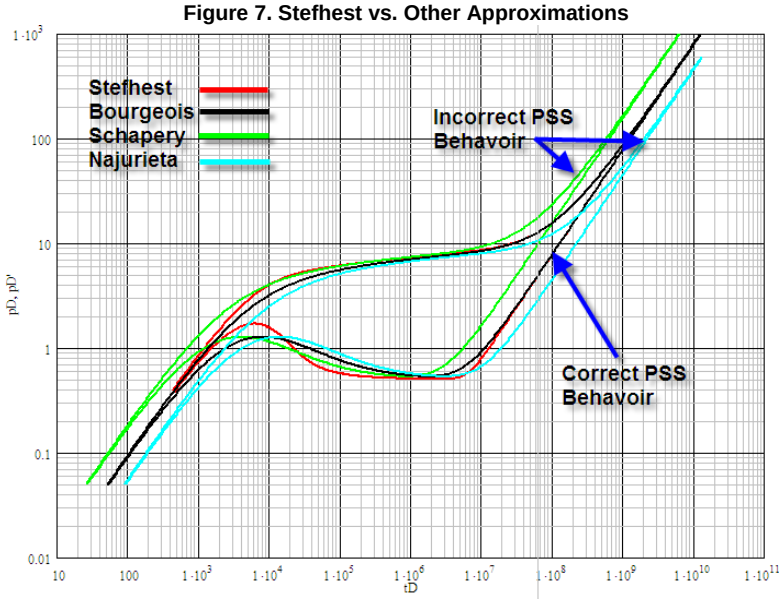

Figure 8. Desuperposition Applicabilitiy to Heterogeniety (Composite)

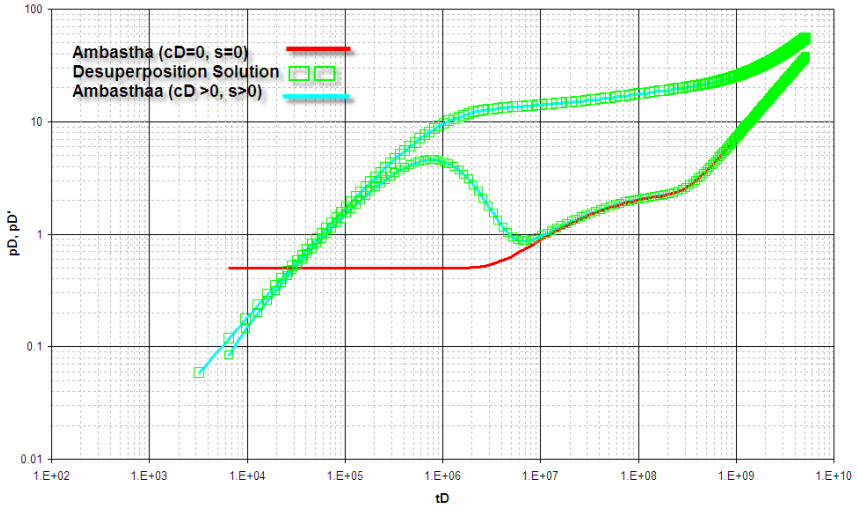

Figure 9. Comparison of Explicit & Approx. Comp. Models

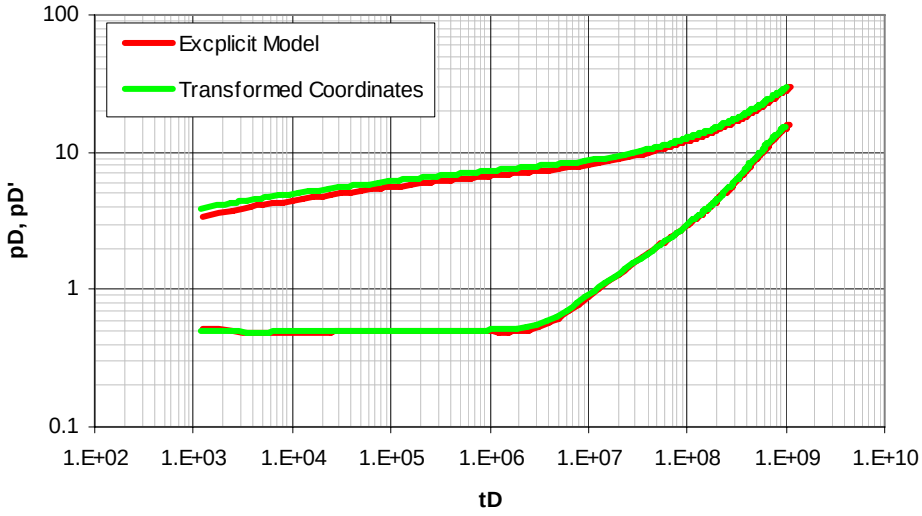

Figure 10. Comparison of Explicit & Approx. Comp. Models

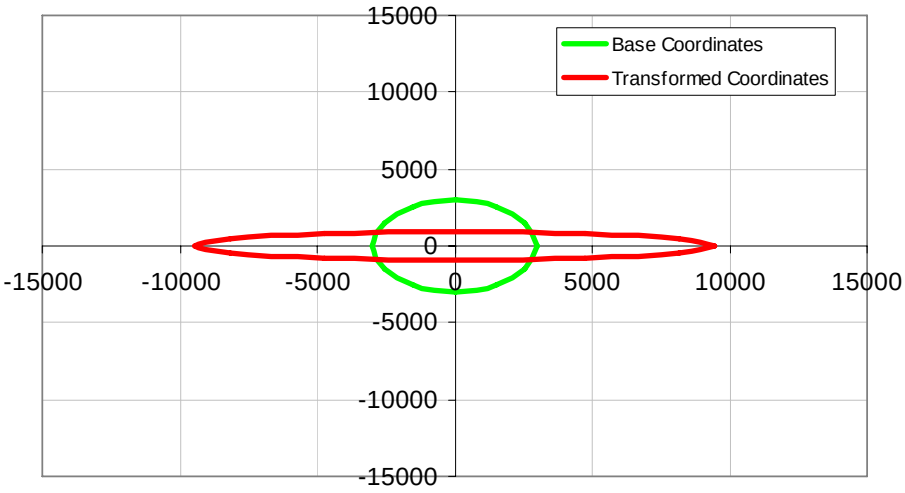

Figure 11. Comparison of Explicit & Approx. Comp. Models

	Zone 1	Zone 2		Known's
Boundary Test Points Zone 1	Normal Pressure Due Zone 2 Image Wells	0	=	Normal Pressure Due to Zone 1 Real Wells
Boundary Test Points Zone 2	0	Normal Pressure Due Zone 2 Image Wells	=	Normal Pressure Due to Zone 2 Real Wells
Interface Test Points	Pressure Due to Zone 1 Image Wells	Pressure Due to Zone 2 Image Wells	=	Pressure Due to Zone 1 Real Wells + Zone 2 Real Wells
	Flux Due Zone 1 Image Wells	Flux Due Zone 2 Image Wells	=	Flux Due to Zone 1 Real Wells + Zone 2 Real Wells

Figure 12. Effect of the Lens Shape and Well Position

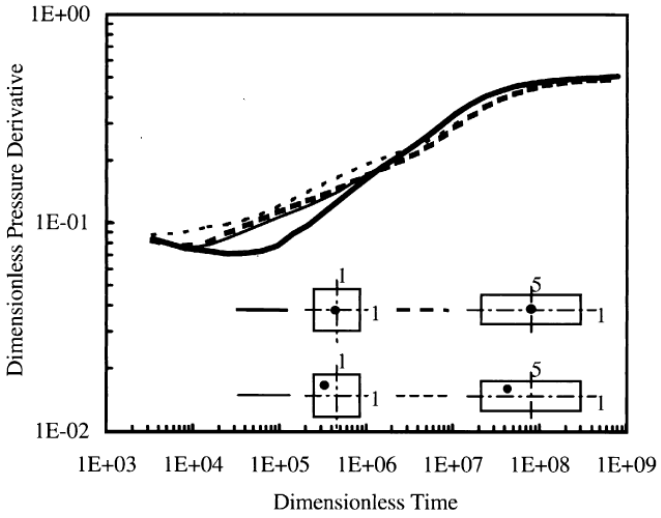

Figure 13. Comparison of Explicit & Approx. Comp. Models

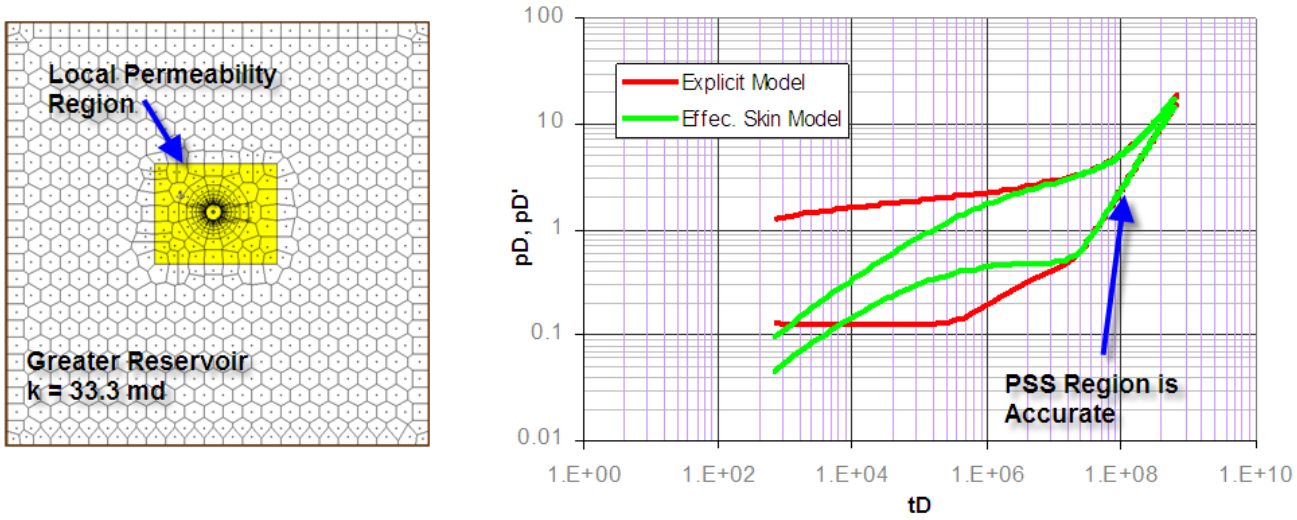

Figure 14. Comparison of Explicit & Approx. Comp. Models

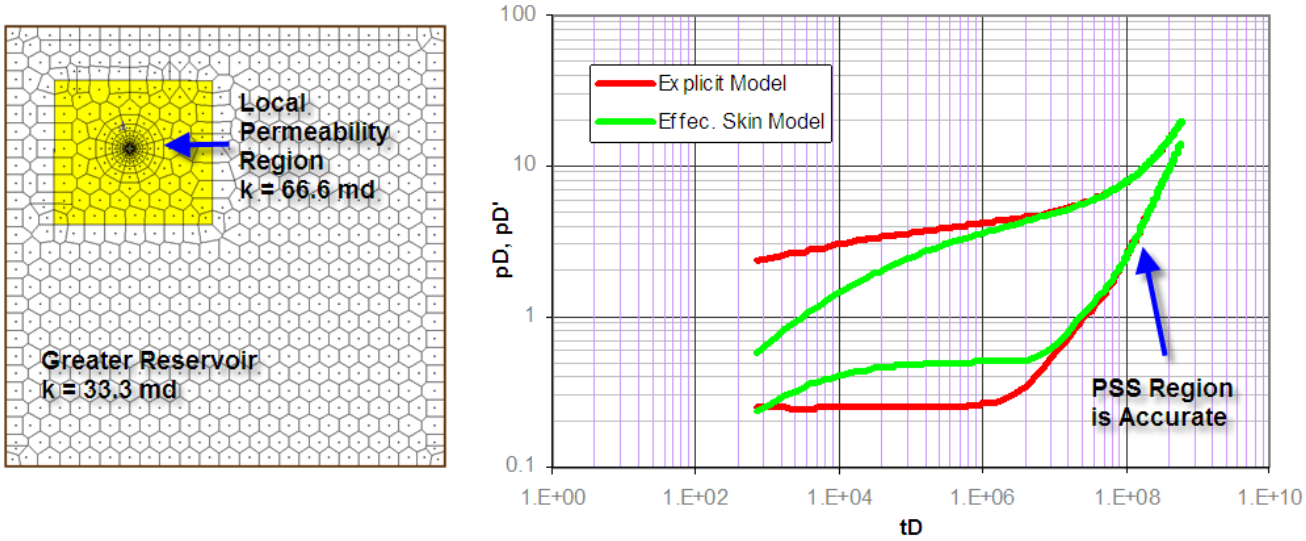

Figure 15. Comparison of Explicit & Approx. Comp. Models

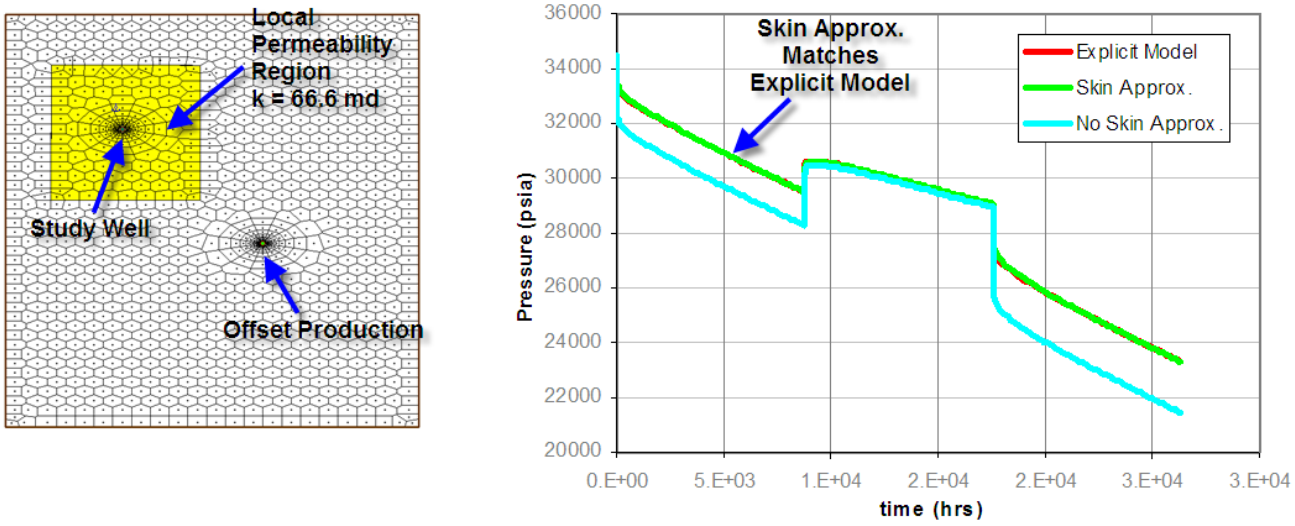

Figure 16. Comparison of Explicit & Approx. Comp. Models

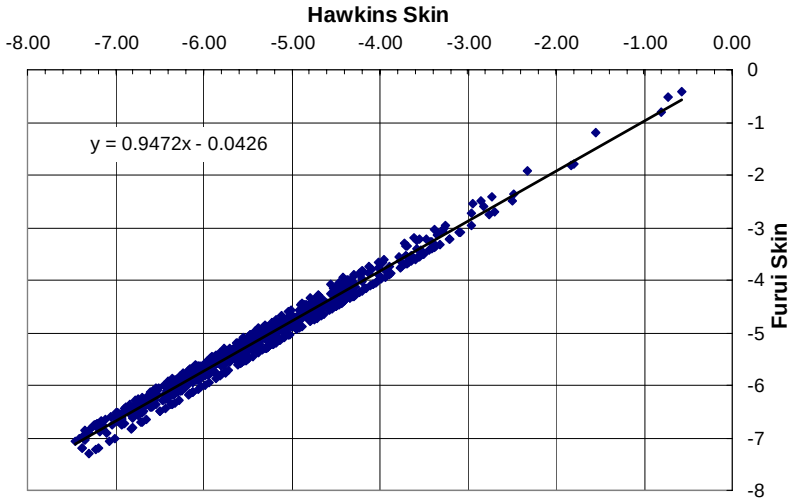

Figure 17. Comparison of Explicit & Approx. Comp. Models

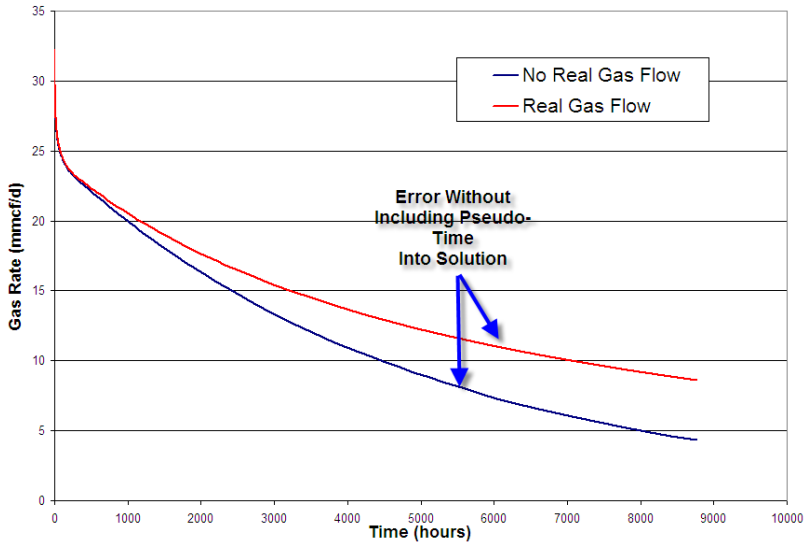

Figure 18. Comparison of Explicit & Approx. Comp. Models

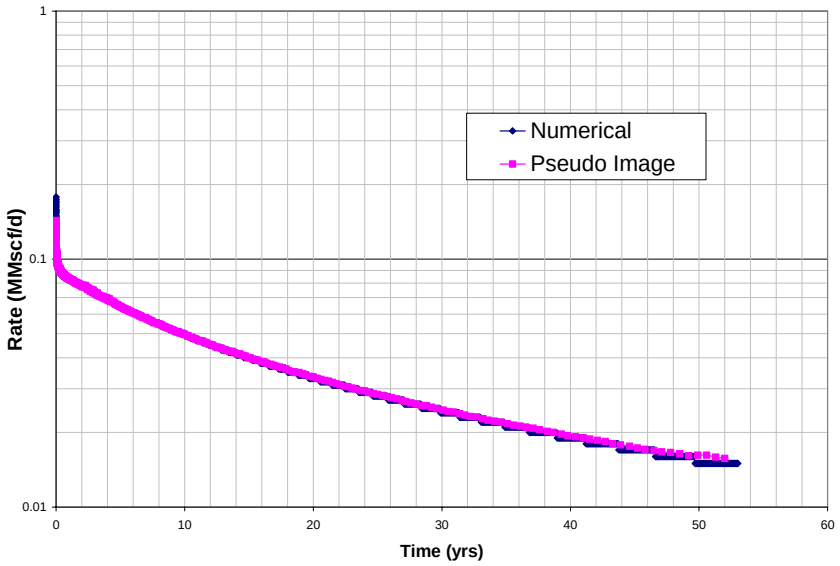

Figure 19. Comparison of Explicit & Approx. Comp. Models

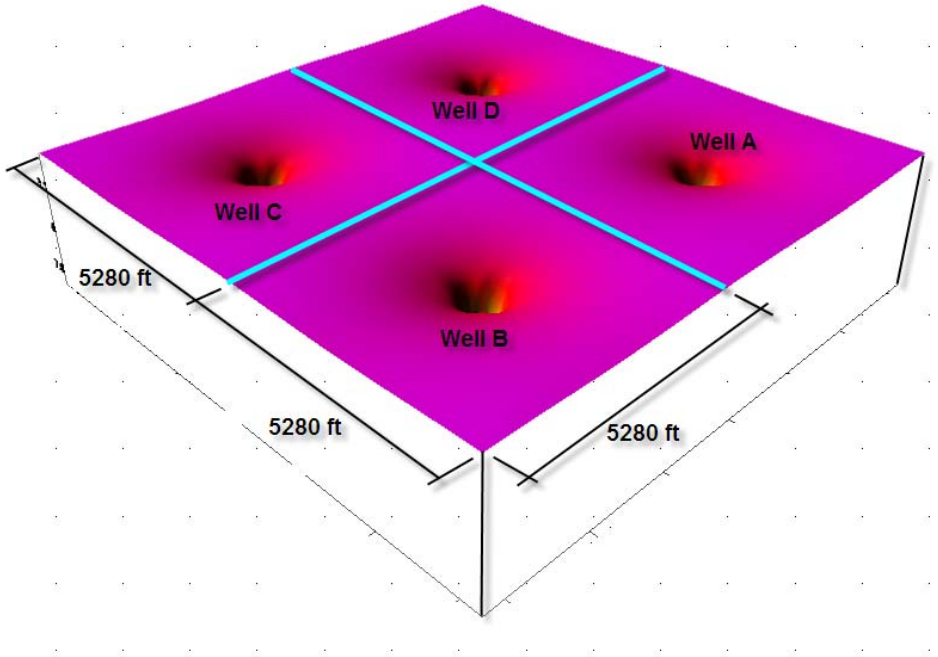

Figure 20. Pressure Drawdown for Symmetrical 4 Well Reservoir Case and Single Well in ¼ Reservoir

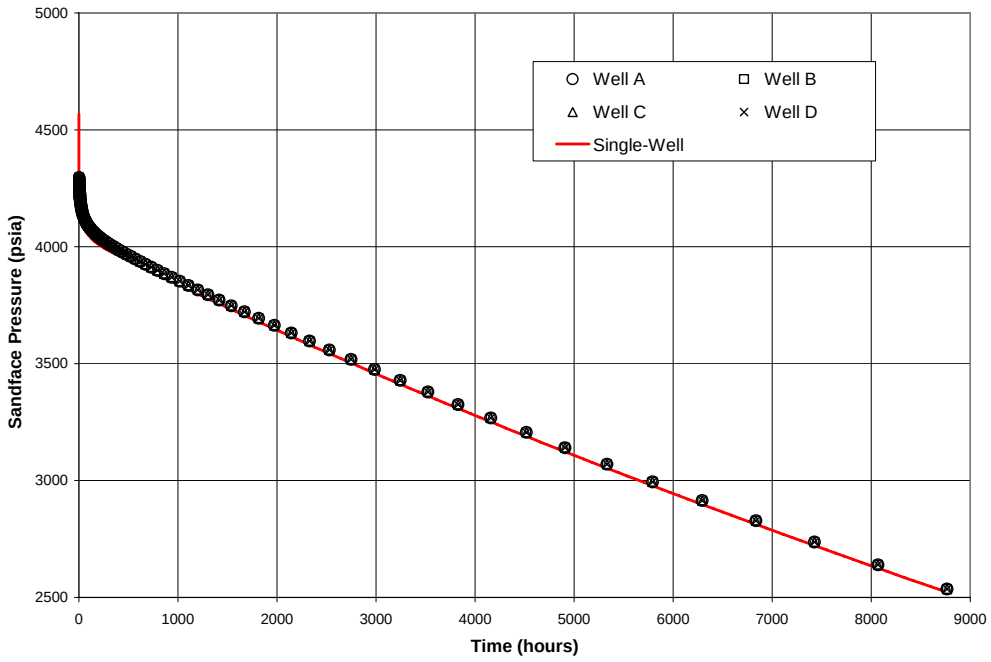

Figure 22. Streamline (Pressure Vector Map) for Symmetrical 4 Well Reservoir

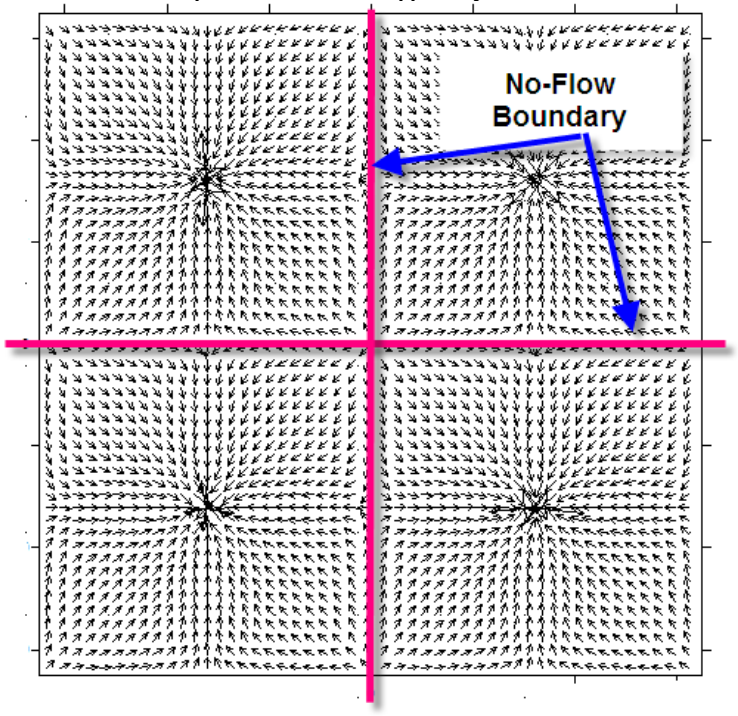

Figure 22 Comparison of 4 Well and Single Well Models